Electronic Supplementary Material (ESI) for ChemComm.

A Proton-conducting Lanthanide Metal-Organic Framework Integrated with Dielectric Anomaly and Second-order Nonlinear Optical Effect

Xiaoqiang Liang,[a,b‡] Feng Zhang, [a‡] Haixia Zhao,[c] Wei Ye, [b] Lasheng Long,[c] Guangshan Zhu*[a]

[a] State Key Laboratory of Inorganic Synthesis and Preparative Chemistry, College of Chemistry, Jilin University, Changchun 130012, PR China

[b] College of Environmental and Chemical Engineering, Xi'an Polytechnic University, Xi'an 710048, PR China

[c] State Key Laboratory of Physical Chemistry of Solid Surface and Department of Chemistry, College of Chemistry and Chemical Engineering, Xiamen University, Xiamen 361005, PR China;

‡ These authors contributed equally to this work.

Experimental Procedures:

Materials and General Procedures

All chemicals were of reagent grade and used as purchased without further purification. The bridging ligand (3R,3'R,3"R)-1,1',1"-(1,3,5-triazine-2,4,6-triyl) -tripiperidine-3-carboxylic acid (R-H_3ttpc) was prepared according to the literature method.[1] Elemental analyses for C, H, and N were taken on a CHN-O-Rapid analyzer and an Elementar Vario MICRO analyzer. The IR spectrum was recorded on a Bruker IF66F/V Fourier transform infrared spectrometer with KBr discs in the 4000 – 400 cm^{-1} range. The solid state vibrational circular dichroism (VCD) and the corresponding IR adsorption spectrum were performed on a Bruker PMA50 spectrometer by using KBr pellets in the 1800 – 1200 cm^{-1} range. Thermogravimetric analysis was carried out on a Perkin-Elmer TGA 7 thermogravimetric analyzer from 25 to 785 °C with a heating rate of 20 °C/min in air. The powder X-ray diffraction (PXRD) analysis of bulk crystals as well as dehydrated and rehydrated samples were measured on a Rigaku diffractometer at a scanning rate of 6º min^{-1} in the 2θ range from 4º to 40º, with graphite monochromatized Cu K_α radiation (λ = 1.5418 Å). The second-order nonlinear optical activity was estimated by measuring a powder sample relative to urea. A pulsed Q-switched Nd:YAG laser at a wavelength of 1064 nm was used to generate a SHG signal from powder samples. The backscattered SHG light was collected by a spherical concave mirror and passed through a filter that transmits only 532 nm radiation.

Preparations

Preparation of single crystals of $\{[Gd_4(R\text{-}ttpc)_2(R\text{-}Httpc)_2(HCOO)_2(H_2O)_8]\cdot 4H_2O\}_n$ (JUC-125): A mixture of $Gd(NO_3)_3\cdot 6H_2O$ (11 mg, 0.025 mmol), R-H_3ttpc (11 mg, 0.025 mmol), HNO_3(2M, 200 μL), DMF(2 mL), and H_2O (3 mL) was placed in a Teflon-capped scintillation vial (20 mL). The mixture was sonicated for 10 min and heated to 100 ºC for 3 days, and then the colorless rod-like crystals of **JUC-125** were

formed. These crystals were collected after washing with distilled water and drying in air (yield: 60% based on R-H_3ttpc ligand). Anal. Calc. for $C_{86}H_{136}N_{24}O_{40}Gd_4$: C, 37.21; H, 4.93; N, 12.11. Found: C, 37.37; H, 4.92; N, 12.17%. IR (KBr, cm^{-1}): 3407(br), 2996(w), 2926(m), 2855(m), 1682(m), 1589(vs), 1540(vs), 1536(vs), 1489(m), 1444(m), 1432(s), 1420(s), 1395(m), 1373(m), 1349(w), 1334(w), 1308(m), 1293(w), 1279(w), 1268(m), 1230(m), 1218(m), 1193(m), 1137(w), 1082(m), 1002(m), 946(w), 847(w), 810(m), 771(m), 737(w), 670(w), 645(w), 614(w), 591(w).

X-ray Structure Determinations

The crystal structure of **JUC-125** was performed on a Bruker SMART APEX CCD diffractometer using graphite monochromatized Mo K_α radiation (λ = 0.71073 Å) at 291(2) K.[2] The raw data was reduced and corrected for Lorentz and polarization effect using the SAINT program and for absorption using the SADABS program. The structure was solved by direct methods and refined with the full-matrix least-squares technique using SHELXTL version 5.1.[3] Anisotropic thermal parameters were refined for all non-hydrogen atoms. Hydrogen atoms were placed in calculated positions calculated positions and refined riding on their parent atoms. The crystallographic data is given in Table S1. Selected bond lengths and bond angles are listed in Table S2. The corresponding H-bond data are presented in Table S3.

Dielectrics

The temperature dependences of dielectric constant and dielectric loss of compressed powder samples of **JUC-125** with 1.86 mm × 1.57 mm × 0.32 mm were measured by 6500B precision impedance analyzer in the frequency range of 10^2 – 10^7 Hz.

Water and nitrogen adsorptions

Water and nitrogen adsorptions' measurements of **JUC-125** were carried out on an Autosorb iQ2 adsorp-tometer, Quantachrome Instruments and their isotherms were recorded. Before the measurements of water and nitrogen adsorptions, **JUC-125** was degassed at 423 K for 12 h, as well as the measurement was carried out at 298 K and 77 K, respectively.

Proton conductivity

Pellets with 13 mm in diameter and 0.85 – 0.95 mm thick were prepared by pressing material (about 220 mg) at 40 kN cm^{-2}. The proton conductivity of the sample was measured by a quasi-four- electrode AC impedance method from 1 Hz to 1 MHz,10 mV ac perturbation and 0.0 V dc rest voltage using a PARSTAT 2273 potentiostat (Princeton Applied Research, EG&GPARC, Princeton, NJ). The samples were covered with silver paint to improve contact with the two copper blocking electrodes in a measurement cell. During the measurement, the measuring cell with the samples were placed in several closed chambers with different relative humidity (RH) levels generated by the different saturated salt solutions. These humidity chambers were made of glass having 19 cm height and 6 cm diameter. The four different standard saturated aqueous salt solutions of $MgCl_2$ (~33 % RH), $Mg(NO_3)_2$ (~53 % RH), NaCl (~75 % RH) and K_2SO_4 (~97 % RH) were used to act as humidity source.[4] The saturated salt solutions were placed in the chambers for 3 days to ensure that the air in the bottle reached to equilibrium state in our investigations. The temperature recorded in close proximity to the sample with a K-type thermocouple in order to measure the temperature dependence of the conductivity. The testing temperature of impedance studies was controlled by the water vapor from 282 to 323 K.

Electrochemical Impedance Spectroscopy (EIS) was used to evaluate the proton resistivity for the sample. The resulting response was displayed in the form of a Nyquist plot. The proton conductivity (σ, S cm^{-1}) was calculated by the following equation: $\sigma = L/RA$, where σ is proton conductivity in S cm^{-1}, L (cm) is the thickness of the sample, A (cm^2) is the area available for proton conduction and R (Ω) is the real part of the impedance response when the imaginary impedance is zero.[5] The measurements have been repeated three times to get reproducible results.

Other Characterization Results and Discussions:

Thermogravimetric Analysis (TGA) and Powder X-ray Diffraction (PXRD)

The thermal stability of **JUC-125** was investigated by using thermogravimetric analysis (TGA) and powder X-ray diffraction (PXRD) measurement. TGA curve of as-synthesized **JUC-125** is presented in Fig. S7. The TGA curve displays that the weight loss of the crystalline and coordinated water molecules occurs in the temperature range of 50 – 180 ºC (observed: 8.51%, calculated: 7.78%). The expulsion of the water molecules up to a high temperature is caused by the strong hydrogen-bonding interactions among carboxyl, carboxylate, the coordinated and lattice water molecules. The collapse of the residual framework begins beyond 250 ºC, attributed to the combustion and decomposition of organic ligands. The phase purity of **JUC-125** was proved by PXRD. As shown in Fig. S8, the experimental pattern is coincident with the simulated one derived from X-ray crystal data. Additionally, the diffraction spectra of **JUC-125** after dehydration and rehydration (Fig. S8c and d) are also identical to that of as-synthesized sample, indicating that the original framework of **JUC-125** is intact after removal and re-adsorption of water molecules.

Vibrational Circular Dichrosim (VCD) Spectroscopy

VCD spectroscopy is described as an effective approach to determine structural information of chiral molecules in the infrared region.[6] Solid-state IR and VCD spectra of crystals of **JUC-125** have been measured by using KBr pellets in the 1700–1200 cm^{-1} range (Fig. S9). In the IR spectra, **JUC-125** shows the characteristic bands of the carboxyl groups for stretch vibrations at 1682 cm^{-1}. The bands at 1395, 1420, 1432, 1444, 1536, 1540, 1589 cm^{-1} arise from stretch vibrations of carboxylate groups. The bands at 1308, 1334, 1349, 1373, 1489 cm^{-1} are attributed to skeleton vibrations of the aromatic ring. The bands at 1218, 1230, 1268, 1279, 1293 cm^{-1} are assigned to C–H bending vibrations. The experimental VCD bands correspond to stretch vibrations of carboxyl groups (1665 – 1694 cm^{-1}), stretch vibrations of carboxylate groups (1389 – 1472 cm^{-1} and 1508 – 1659 cm^{-1}), skeleton vibrations of the aromatic ring (1297 – 1374 cm^{-1} and 1471 – 1502 cm^{-1}), and C–H bending vibrations (1206 – 1295 cm^{-1}), respectively. The sample shows distinct signals in relation to IR absorption peaks, in which positive or negative cotton effects indicate

that the crystals of **JUC-125** are chirality.

Water and Nitrogen Adsorptions

Water adsorption and desorption isotherms of **JUC-125** was evaluated at 298 K to better understand the proton conduction mechanism. As depicted in Fig. S13, water uptake of the evacuated **JUC-125** presents a continuously growing trend with increasing RH. The water content of **JUC-125** at about 97% RH is 141.6 mg g^{-1}, corresponding to 20.1 water molecules per formula unit. It is significantly larger than the initial number of water molecules in **JUC-125** (12 water molecules), implying that channels are hydrophilic and capable of enclosing external water molecules. The additional 8.1 water molecules in **JUC-125** are responsible for high proton conduction under high RH. The desorption process exhibits a large hysteresis, which may be due to strong hydrogen-bonding interaction between water molecules and host framework as well as the chemisorption of water molecules on available Gd coordination sites.[7]

Nitrogen adsorption and desorption experiments of **JUC-125** have been carried out. However, JUC-125 almost shows no adsorption behavior. This may be due to no removal of coordinated formatted ions by thermal activation and still occupation in the 1D rectangular channel.

Elementary Analysis (EA) and TGA of the Activated Sample

The Elementary Analysis (EA) and TGA of the activated sample have been carried out and the data are shown in Table S4 and Fig. S15. The data of EA illustrates that the water content of the activated sample is almost consistent with the pristine sample. The TGA curve of the activated sample also displays that the weight loss of the crystalline and coordinated water molecules occurs in the temperature range of about 50 – 180 ºC (observed: 7.33%). The above results show that the activated sample captures about 8 coordination water molecules and 4 guest water molecules and is almost identical to the original sample. The strong water uptake under the ambient humidity is likely attributed to the chemisorption of water molecules on available Gd coordination sites as well as strong hydrogen-bonding interactions between host

framework and water molecules.

Relationship between Proton Conductivity and Coordination Water Molecules

The measurement of humidity-dependent proton conductivity suggests that proton conductivity is closely correlated to the number of water molecules encapsulated in channels, including coordination water molecules and guest water molecules. There is a gradual decrease in the conductivity as the number of coordination water molecules is reduced. Because proton-conducting pathway formed by coordination water molecules plays an important role in proton transport.

Reference

1. X. L. Zhao, H. Y. He, T. P. Hu, F. N. Dai and D. F. Sun, *Inorg. Chem.*, 2009, **48**, 8057.
2. SMART and SAINT. *Area Detector Control and Integration Software*; Siemens Analytical X-Ray Systems, Inc.: Madison, WI, 1996.
3. G. M. Sheldrick, *SHELXTL V5.1 Software Reference Manual*; Bruker AXS, Inc.: Madison, WI, 1997.
4. Z. Li, Q. Zhang, H. Liu, P. He, X. Xu and J. Li, *J. Power Sources*, 2006, **158**, 103.
5. E. Jaimez, G. B. Hix and R. C. T. Slade, *J. Mater. Chem.* 1997, **7**, 475.
6. (a) G. Tian, G. S. Zhu, X. Y. Yang, Q. R. Fang, M. Xue, J. Y. Sun, Y. Wei and S. L. Qiu, *Chem. Commun.*, 2005, **41**, 1396; (b) Y. Ma, Z. B. Han, Y. K. He and L. G. Yang, *Chem. Commun.*, 2007, **43**, 4107; (c) W. G. Lu, J. Z. Gu, L. Jiang, M. Y. Tan and T. B. Lu, *Cryst. Growth Des.* 2008*,* **8***,* 192.
7. P. Küsgens, M. Rose, I. Senkovska, H. Fröde, A. Henschel, S. Siegle and S. Kaskel, *Micropor. Mesopor. Mater.*, 2009, **120**, 325.

Table S1 Crystallographic data and details of refinements for **JUC-125**

Complex	**JUC-125**
Empirical formula	$C_{86}H_{136}Gd_4N_{24}O_{40}$
*M*r	2775.19
Crystal system	Monoclinic
Space group	$P2_1$
a (Å)	9.1427(7)
b (Å)	24.503(2)
c (Å)	24.588(2)
α (°)	90
β (°)	91.0890(10)
γ (°)	90
V (Å^3)	5507.3(8)
Z	2
D_c (g/m^{-3})	1.674
μ (mm^{-1})	2.471
θ range [º]	0.83 − 26.00
Collected reflections	30445
Unique reflections	19953
Parameters	1387
F(000)	2792
T (K)	291(2)
R_1 [a], wR_2[b] [I > 2σ (I)]	0.0720, 0.1989
R_1 [a], wR_2 [b] [all data]	0.0832, 0.2067
GOF	1.014
Largest peak and hole (e ·Å^{-3})	2.668, -2.679
Flack parameter	0.046(15)

[a] $R_1 = \sum||F_o|-|F_c||/\sum|F_o|$. [b] $wR_2 = [\sum w(|F_o^2|-|F_c^2|)^2/\sum w(|F_o^2|)^2]^{1/2}$.

Table S2 Selected bond lengths (Å) and angles (°) for **JUC-125**

Complex **JUC-125**

Gd(1)−O(24c)	2.312(11)	Gd(1)−O(22a)	2.390(10)
Gd(1)−O(14)	2.401(9)	Gd(1)−O(3W)	2.416(9)
Gd(1)−O(2W)	2.426(9)	Gd(1)−O(1W)	2.461(10)
Gd(1)−O(21a)	2.465(10)	Gd(1)−O(2)	2.510(9)
Gd(1)−O(1)	2.665(9)	Gd(2)−O(1)	2.293(9)
Gd(2)−O(27)	2.374(10)	Gd(2)−O(23c)	2.381(9)
Gd(2)−O(13)	2.398(10)	Gd(2)−O(4W)	2.403(8)
Gd(2)−O(7)	2.454(10)	Gd(2)−O(8)	2.533(11)
Gd(2)−O(10d)	2.613(9)	Gd(2)−O(14)	2.636(9)
Gd(3)−O(19)	2.327(9)	Gd(3)−O(12e)	2.382(10)
Gd(3)−O(25)	2.390(10)	Gd(3)−O(18)	2.397(10)
Gd(3)−O(8W)	2.400(9)	Gd(3)−O(4f)	2.411(10)
Gd(3)−O(15b)	2.556(9)	Gd(3)−O(17)	2.593(10)
Gd(3)−O(11e)	2.628(10)	Gd(4)−O(3f)	2.312(12)
Gd(4)−O(11e)	2.360(10)	Gd(4)−O(6W)	2.374(10)
Gd(4)−O(5W)	2.404(10)	Gd(4)−O(5b)	2.431(9)
Gd(4)−O(20)	2.501(9)	Gd(4)−O(7W)	2.502(11)
Gd(4)−O(6b)	2.505(10)	Gd(4)−O(19)	2.663(8)
O(24c)−Gd(1)−O(22a)	77.5(3)	O(24c)−Gd(1)−O(14)	76.6(3)
O(22a)−Gd(1)−O(14)	89.1(3)	O(24c)−Gd(1)−O(3W)	137.9(3)
O(22a)−Gd(1)−O(3W)	132.2(3)	O(14)−Gd(1)−O(3W)	75.3(3)
O(24c)−Gd(1)−O(2W)	139.7(3)	O(22a)−Gd(1)−O(2W)	93.1(3)
O(14)−Gd(1)−O(2W)	143.1(3)	O(3W)−Gd(1)−O(2W)	76.1(3)
O(24c)−Gd(1)−O(1W)	70.4(3)	O(22a)−Gd(1)−O(1W)	71.0(3)
O(14)−Gd(1)−O(1W)	144.2(3)	O(3W)−Gd(1)−O(1W)	139.9(3)
O(2W)−Gd(1)−O(1W)	69.6(3)	O(24c)−Gd(1)−O(21a)	124.6(3)
O(22a)−Gd(1)−O(21a)	52.9(3)	O(14)−Gd(1)−O(21a)	79.4(3)
O(3W)−Gd(1)−O(21a)	79.7(3)	O(2W)−Gd(1)−O(21a)	73.0(3)
O(1W)−Gd(1)−O(21a)	108.4(3)	O(24c)−Gd(1)−O(2)	88.9(4)
O(22a)−Gd(1)−O(2)	146.5(3)	O(14)−Gd(1)−O(2)	117.7(3)
O(3W)−Gd(1)−O(2)	77.2(3)	O(2W)−Gd(1)−O(2)	77.5(3)
O(1W)−Gd(1)−O(2)	75.6(3)	O(21a)−Gd(1)−O(2)	146.1(3)
O(24c)−Gd(1)−O(1)	70.7(3)	O(22a)−Gd(1)−O(1)	143.8(3)
O(14)−Gd(1)−O(1)	67.4(3)	O(3W)−Gd(1)−O(1)	69.8(3)
O(2W)−Gd(1)−O(1)	122.3(3)	O(1W)−Gd(1)−O(1)	112.4(3)
O(21a)−Gd(1)−O(1)	139.2(3)	O(2)−Gd(1)−O(1)	50.8(3)
O(1)−Gd(2)−O(27)	76.0(4)	O(1)−Gd(2)−O(23c)	73.2(3)
O(27)−Gd(2)−O(23c)	138.0(3)	O(1)−Gd(2)−O(13)	118.7(3)
O(27)−Gd(2)−O(13)	81.6(4)	O(23c)−Gd(2)−O(13)	88.9(4)
O(1)−Gd(2)−O(4W)	144.4(3)	O(27)−Gd(2)−O(4W)	78.4(3)
O(23c)−Gd(2)−O(4W)	140.4(3)	O(13)−Gd(2)−O(4W)	81.0(3)
O(1)−Gd(2)−O(7)	102.5(4)	O(27)−Gd(2)−O(7)	143.0(3)
O(23c)−Gd(2)−O(7)	72.2(3)	O(13)−Gd(2)−O(7)	127.3(4)
O(4W)−Gd(2)−O(7)	83.8(3)	O(1)−Gd(2)−O(8)	138.6(4)
O(27)−Gd(2)−O(8)	144.9(3)	O(23c)−Gd(2)−O(8)	68.4(3)
O(13)−Gd(2)−O(8)	75.6(4)	O(4W)−Gd(2)−O(8)	72.0(3)

O(7)−Gd(2)−O(8)	51.7(3)	O(1)−Gd(2)−O(10d)	79.9(3)
O(27)−Gd(2)−O(10d)	72.0(3)	O(23c)−Gd(2)−O(10d)	128.1(3)
O(13)−Gd(2)−O(10d)	143.0(3)	O(4W)−Gd(2)−O(10d)	68.8(3)
O(7)−Gd(2)−O(10d)	71.4(3)	O(8)−Gd(2)−O(10d)	112.7(3)
O(1)−Gd(2)−O(14)	69.3(3)	O(27)−Gd(2)−O(14)	71.3(3)
O(23c)−Gd(2)−O(14)	71.5(3)	O(13)−Gd(2)−O(14)	49.5(3)
O(4W)−Gd(2)−O(14)	124.1(3)	O(7)−Gd(2)−O(14)	143.7(3)
O(8)−Gd(2)−O(14)	110.7(3)	O(10d)−Gd(2)−O(14)	136.6(3)
O(19)−Gd(3)−O(12e)	119.1(3)	O(19)−Gd(3)−O(25)	77.3(3)
O(12e)−Gd(3)−O(25)	79.2(4)	O(19)−Gd(3)−O(18)	108.4(3)
O(12e)−Gd(3)−O(18)	123.7(3)	O(25)−Gd(3)−O(18)	142.7(3)
O(19)−Gd(3)−O(8W)	142.7(3)	O(12e)−Gd(3)−O(8W)	79.7(3)
O(25)−Gd(3)−O(8W)	75.3(3)	O(18)−Gd(3)−O(8W)	80.3(3)
O(19)−Gd(3)−O(4f)	75.3(3)	O(12e)−Gd(3)−O(4f)	91.6(4)
O(25)−Gd(3)−O(4f)	141.8(3)	O(18)−Gd(3)−O(4f)	72.2(3)
O(8W)−Gd(3)−O(4f)	139.7(3)	O(19)−Gd(3)−O(15b)	77.7(3)
O(12e)−Gd(3)−O(15b)	145.4(4)	O(25)−Gd(3)−O(15b)	75.5(3)
O(18)−Gd(3)−O(15b)	70.1(3)	O(8W)−Gd(3)−O(15b)	71.3(3)
O(4f)−Gd(3)−O(15b)	122.8(3)	O(19)−Gd(3)−O(17)	141.0(3)
O(12e)−Gd(3)−O(17)	73.5(4)	O(25)−Gd(3)−O(17)	140.8(3)
O(18)−Gd(3)−O(17)	50.3(3)	O(8W)−Gd(3)−O(17)	72.6(3)
O(4f)−Gd(3)−O(17)	67.3(3)	O(15b)−Gd(3)−O(17)	113.8(3)
O(19)−Gd(3)−O(11e)	68.9(3)	O(12e)−Gd(3)−O(11e)	50.4(3)
O(25)−Gd(3)−O(11e)	70.8(3)	O(18)−Gd(3)−O(11e)	146.3(3)
O(8W)−Gd(3)−O(11e)	123.2(3)	O(4f)−Gd(3)−O(11e)	74.8(3)
O(15b)−Gd(3)−O(11e)	136.5(3)	O(17)−Gd(3)−O(11e)	109.6(3)
O(3f)−Gd(4)−O(11e)	75.2(4)	O(3f)−Gd(4)−O(6W)	139.6(3)
O(11e)−Gd(4)−O(6W)	145.2(3)	O(3f)−Gd(4)−O(5W)	135.6(3)
O(11e)−Gd(4)−O(5W)	75.5(4)	O(6W)−Gd(4)−O(5W)	75.9(3)
O(3f)−Gd(4)−O(5b)	80.5(3)	O(11e)−Gd(4)−O(5b)	87.6(3)
O(6W)−Gd(4)−O(5b)	96.2(3)	O(5W)−Gd(4)−O(5b)	130.4(3)
O(3f)−Gd(4)−O(20)	85.9(4)	O(11e)−Gd(4)−O(20)	117.4(3)
O(6W)−Gd(4)−O(20)	75.4(3)	O(5W)−Gd(4)−O(20)	78.9(4)
O(5b)−Gd(4)−O(20)	147.3(3)	O(11e)−Gd(4)−O(7W)	141.8(3)
O(3f)−Gd(4)−O(7W)	69.9(3)	O(6W)−Gd(4)−O(7W)	70.8(3)
O(5W)−Gd(4)−O(7W)	142.0(3)	O(5b)−Gd(4)−O(7W)	71.9(3)
O(20)−Gd(4)−O(7W)	75.6(3)	O(3f)−Gd(4)−O(6b)	127.8(3)
O(11e)−Gd(4)−O(6b)	81.8(3)	O(6W)−Gd(4)−O(6b)	73.8(3)
O(5W)−Gd(4)−O(6b)	79.3(3)	O(5)−Gd(4)−O(6b)	52.0(3)
O(20)−Gd(4)−O(6b)	145.8(4)	O(7W)−Gd(4)−O(6b)	107.6(3)
O(3f)−Gd(4)−O(19)	71.7(3)	O(11e)−Gd(4)−O(19)	67.8(3)
O(6W)−Gd(4)−O(19)	117.0(3)	O(5W)−Gd(4)−O(19)	66.7(3)
O(5b)−Gd(4)−O(19)	146.5(3)	O(20)−Gd(4)−O(19)	49.6(3)
O(7W)−Gd(4)−O(19)	113.6(3)	O(6b)−Gd(4)−O(19)	138.7(3)

Symmetry codes: a) $-x+1, y-1/2, -z+1$; b) $-x+1, y+1/2, -z+1$; c) $x+1, y, z$; d) $-x+1, y-1/2, -z+2$; e) $x, y, z-1$; f) $x-1, y, z-1$ for **JUC-125**.

Table S3 Hydrogen-bonding geometry parameters (Å, °) for **JUC-125**

Complex **JUC-125**				
D−H···A	d(D-H)	d(H···A)	d(D···A)	<(DHA)
O(9)−H(9)...O(7g)	0.82	1.75	2.552(13)	167.0
O(16)−H(16)...O(18a)	0.82	1.75	2.561(13)	168.1
O(1W)−H(1X)...O(13c)	0.96	2.28	3.218(14)	164.8
O(1W)−H(1Y)...O(8c)	0.96	2.14	2.783(13)	122.7
O(2W)−H(2X)...O(26i)	0.96	2.04	2.713(13)	125.6
O(2W)−H(2Y)...O(4Wc)	0.96	2.46	3.410(13)	170.2
O(3W)−H(3Y)...O(27)	0.96	1.89	2.719(13)	143.3
O(4W)−H(4X)...O(28)	0.96	2.10	2.660(14)	115.4
O(4W)−H(4Y)...O(2h)	0.96	2.21	2.737(13)	113.5
O(5W)−H(5Y)...O(3Wb)	0.96	2.30	2.829(13)	114.2
O(7W)−H(7X)...O(12)	0.96	2.35	3.270(13)	159.5
O(7W)−H(7Y)...O(17h)	0.96	2.14	2.790(13)	123.8
O(8W)−H(8X)...O(20c)	0.96	1.89	2.788(13)	155.4
O(8W)−H(8Y)...O(26)	0.96	1.72	2.643(13)	161.3
O(9W)−H(9X)...O(5j)	0.85	2.35	2.823(14)	115.4
O(9W)−H(9Y)...O(3)	0.97	2.39	3.210(14)	141.7
O(10W)−H(10X)...O(28)	0.85	2.41	2.918(14)	119.4
O(10W)−H(10Y)...O(3Wh)	0.85	2.23	2.785(14)	122.9
O(11W)−H(11X)...O(22k)	0.85	2.12	2.781(15)	133.9
O(11W)−H(11Y)...O(24a)	0.85	2.50	3.206(14)	140.7

Symmetry codes: a) $-x+1, y-1/2, -z+1$; b) $-x+1, y+1/2, -z+1$; c) $x+1, y, z$; g) $-x+1, y+1/2, -z+2$; h) $x-1, y, z$; i) $-x+2, y-1/2, -z+1$; j) $-x+2, y+1/2, -z+1$; k) $x+1, y-1, z$ for **JUC-125**.

Table S4 Elementary Analysis of the activated sample and JUC-125

Sample	C%	H%	N%
JUC-125 (Calculated Value)	37.21	4.93	12.11
JUC-125 (Measured Value)	37.37	4.92	12.17
the activated sample of **JUC-125**	37.38	4.91	12.03

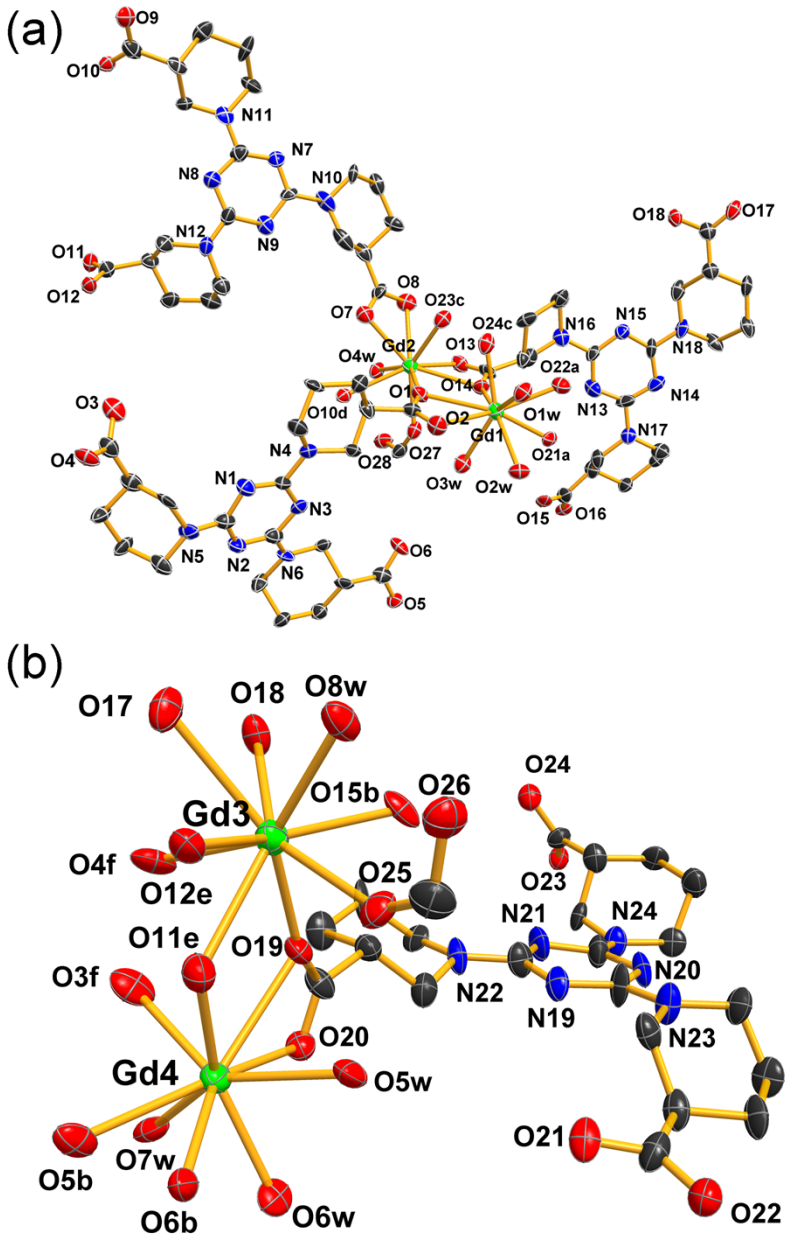

Fig. S1 (a) View of the coordination environments of Gd (III) in **JUC-125**, thermal ellipsoids are drawn at the 50% probability level. Lattice water molecules and hydrogen atoms have been omitted for clarity (Symmetry codes: a) $-x+1, y-1/2, -z+1$; b) $-x+1, y+1/2, -z+1$; c) $x+1, y, z$; d) $-x+1, y-1/2, -z+2$; e) $x, y, z-1$; f) $x-1, y, z-1$) (Black, C; blue, N; Red, O; Green, Gd).

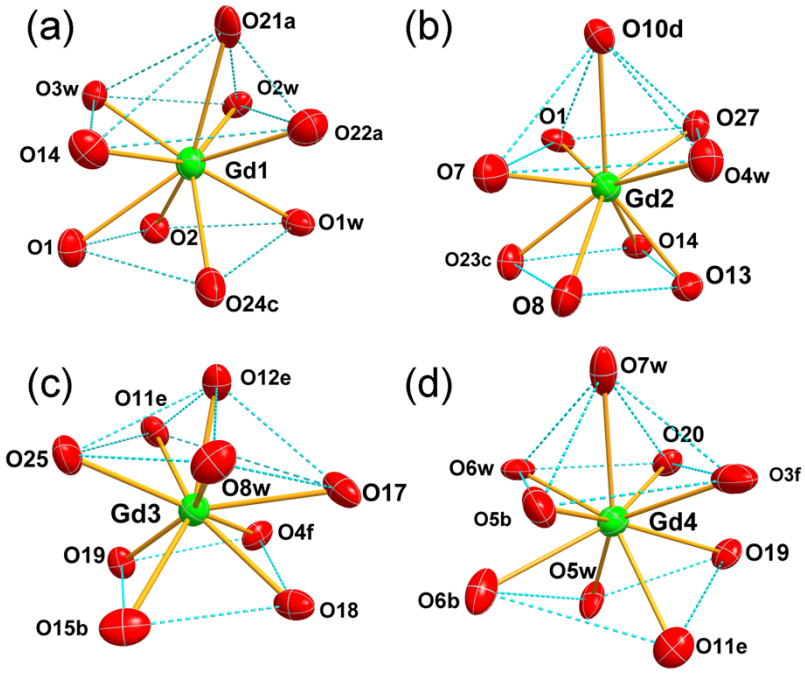

Fig. S2 Local coordination geometry of Gd（III) ions in **JUC-125**. The other atoms have been omitted for clarity (Symmetry codes: a) $-x+1, y-1/2, -z+1$; b) $-x+1, y+1/2, -z+1$; c) $x+1, y, z$; d) $-x+1, y-1/2, -z+2$; e) $x, y, z-1$; f) $x-1, y, z-1$) (Red, O; Green, Gd).

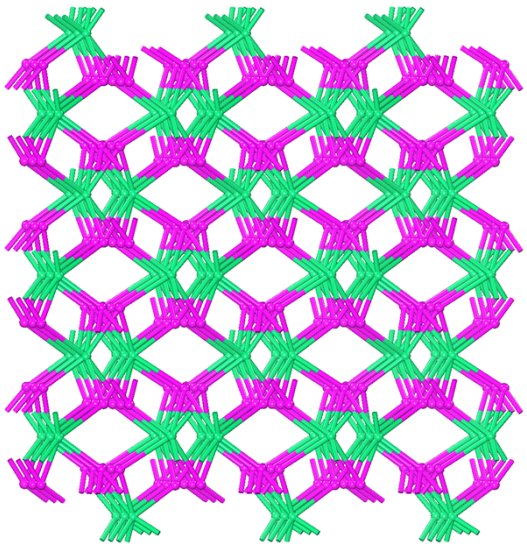

Fig. S3 Schematic description of the (3, 6)-connected 3D network with $(48^2)_2(4^68^710^2)$ topology.

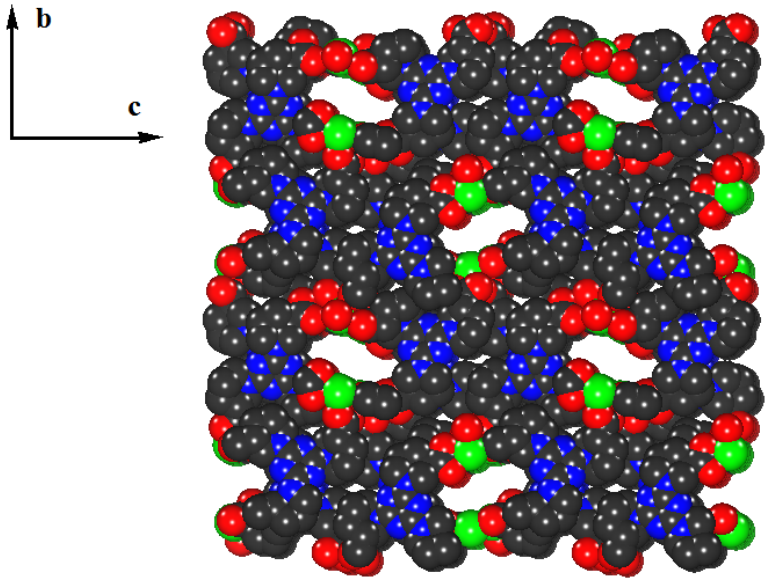

Fig. S4 The 1D rectangular channel with dimensions of ca. 5 × 10 $Å^2$ (Black, C; blue, N; Red, O; Green, Gd).

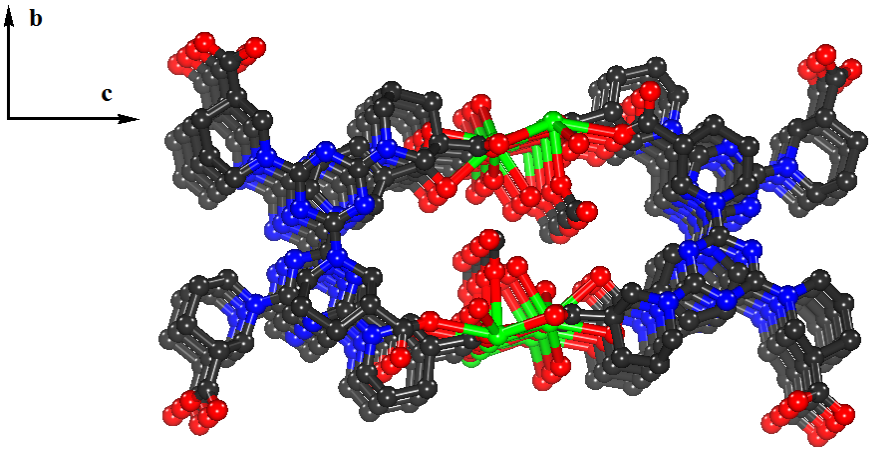

Fig.S5 The hydrophilic channel formed by carboxylate oxygen atoms, coordinated aqua molecules, nitrogen atoms from triazine rings (Black, C; blue, N; Red, O; Green, Gd).

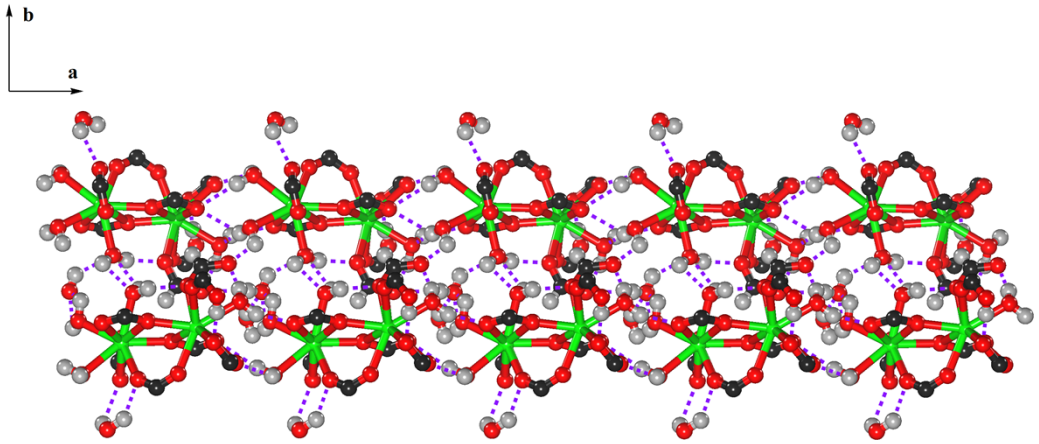

Fig. S6 Three types of hydrogen-bonding interactions in the cavity (Black, C; blue, N; Red, O; Green, Gd; Light Gray, H).

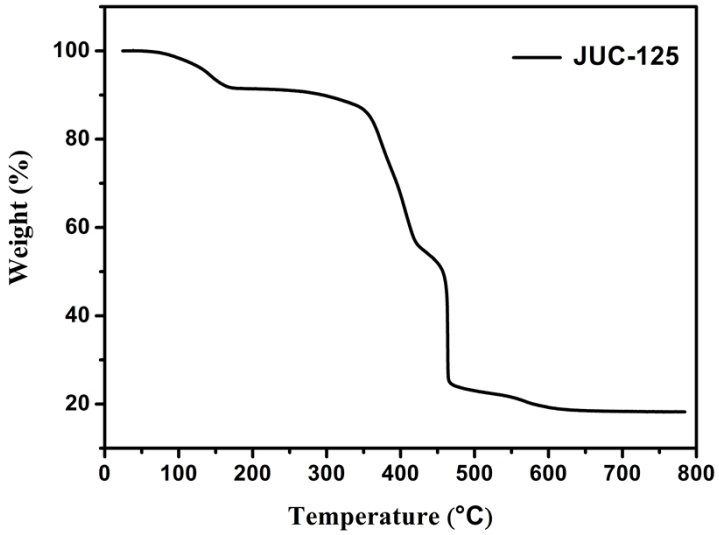

Fig. S7 Thermogravimetric curve for **JUC-125**.

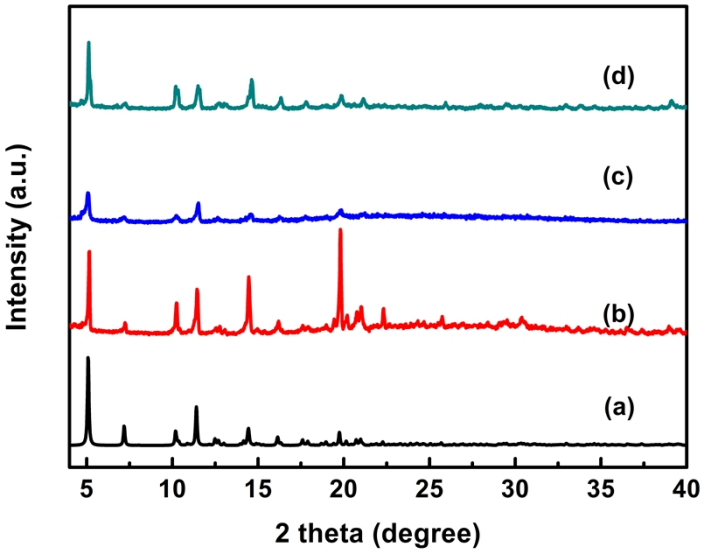

Fig. S8 PXRD patterns of (a) a simulation based on single-crystal analysis of **JUC-125**, (b) as-synthesized bulk crystals of **JUC-125**, (c) activated sample of **JUC-125**, and (d) rehydration sample of **JUC-125**.

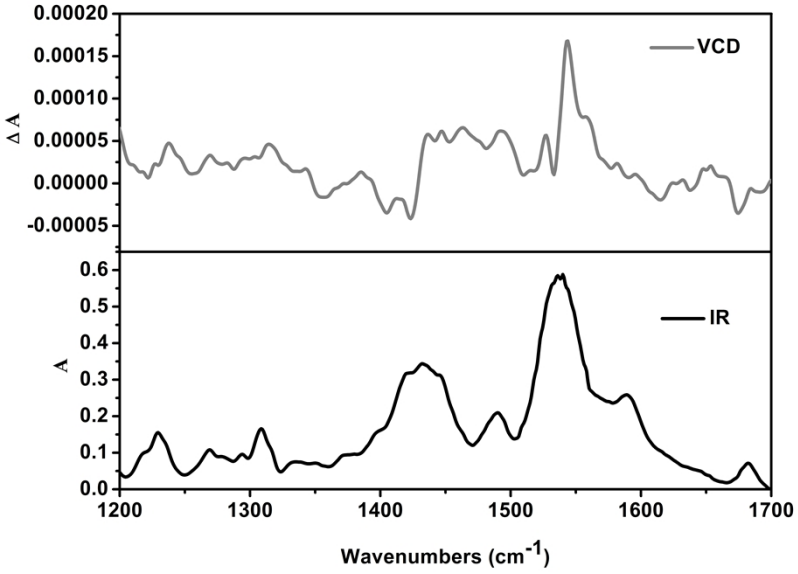

Fig. S9 The VCD (top) and IR absorption spectrum (bottom) of **JUC-125** in the solid state at room temperature.

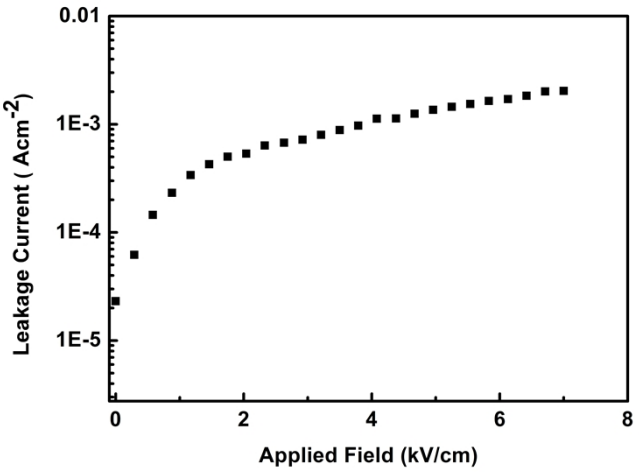

Fig. S10 Plot of leakage current versus electric field for **JUC-125**.

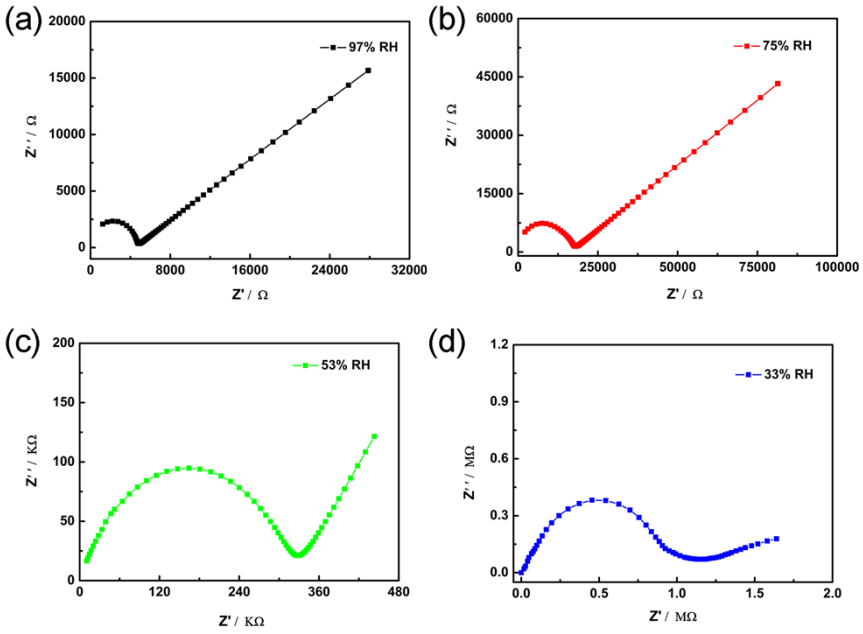

Fig. S11 Nyquist plots of **JUC-125** (a) ~97% RH, (b) ~75% RH, (c)~53% RH and (d) ~33% RH at 298 K.

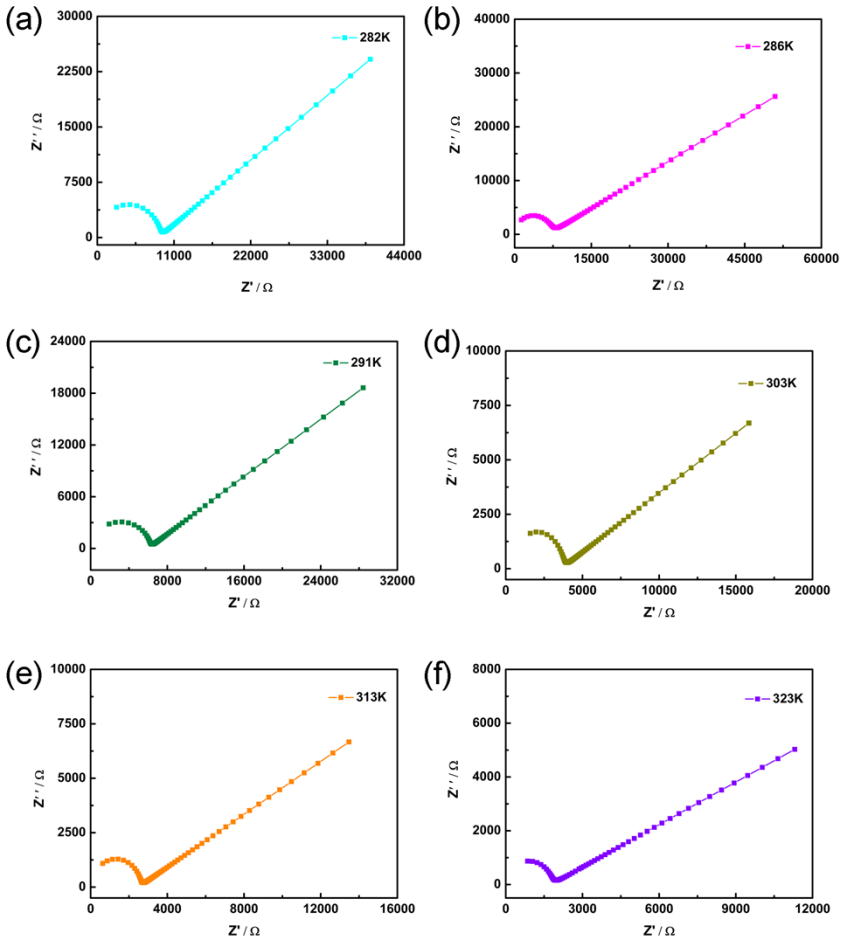

Fig. S12 Nyquist plots of **JUC-125** at different temperatures and ~97% RH (relative humidity).

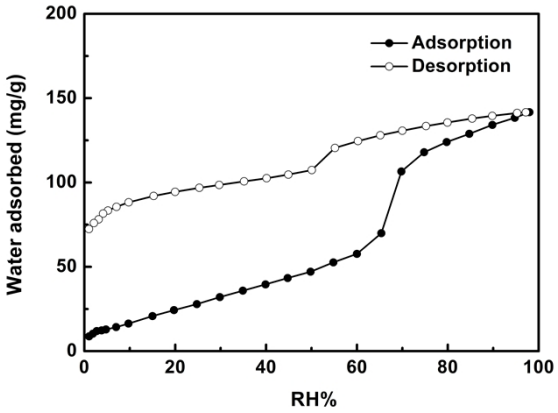

Fig. S13 Water adsorption capacity of **JUC-125** as a function of humidity.

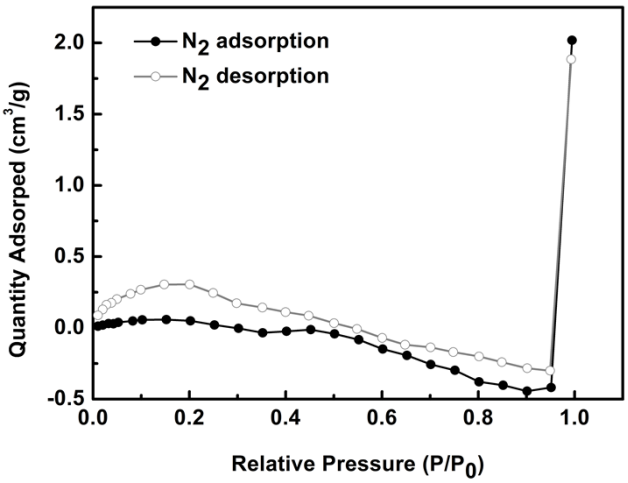

Fig. S14 N_2 sorption isotherm of **JUC-125** at 77 K.

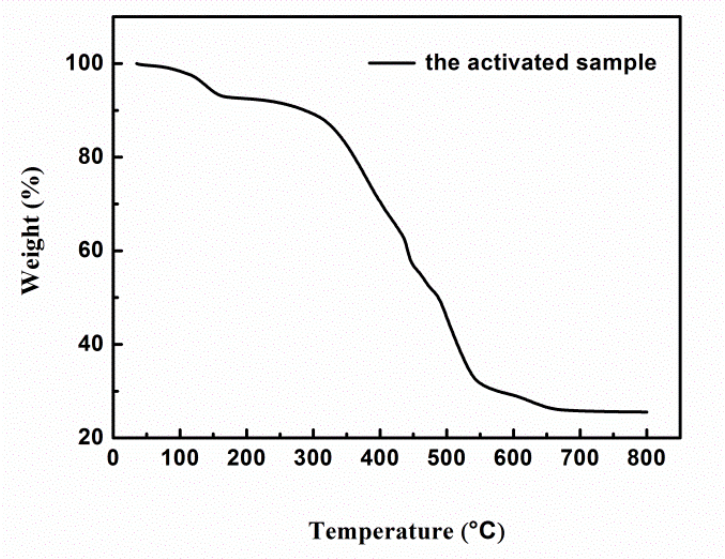

Fig. S15 Thermogravimetric curve for the activated sample.